Seasonal variation in exposure to particulate matter among children attending different levels of education: Comparison of two dosimetry models

Isabella Charres, Yago Cipoli, Leonardo C Furst, Estela D Vicente, Ismael Casotti Rienda, Mihalis Lazaridis, Manuel Feliciano, Célia Alves

Seasonal variation in exposure to particulate matter among children attending different levels of education: comparison of two dosimetry models

Isabella Charres[a], Yago Cipoli[a], Leonardo C. Furst[a], Estela D. Vicente[a], Ismael Casotti Rienda[a], Mihalis Lazaridis[b], Manuel Feliciano[c,d], Célia Alves[a]

[a] Centre for Environmental and Marine Studies (CESAM), Department of Environment, University of Aveiro, 3810-193, Aveiro, Portugal

[b] School of Chemical and Environmental Engineering, Technical University of Crete, 73100, Chania, Greece

[c] Centro de Investigação de Montanha (CIMO), Instituto Politécnico de Bragança, 5300-253, Bragança, Portugal

[d] Laboratório Associado para a Sustentabilidade e Tecnologia em Regiões de Montanha (SusTEC), Instituto Politécnico de Bragança, 5300-253, Bragança, Portugal

Corresponding author:
Isabella Charres Fandino
isabellacharres@ua.pt
Centre for Environmental and Marine Studies (CESAM), Department of Environment, University of Aveiro, 3810-193, Aveiro, Portugal

Abstract

Exposure to particulate matter (PM) has been associated with several adverse health outcomes. Studies indicate that children may be exposed to much higher concentrations of PM at school than in other environments. There exists very little data on the deposited dose of PM while children attend classes. This study was carried out in a school located near an industrial complex in Portugal and attended by children aged 3–12 years. Indoor PM_{10}, $PM_{2.5}$ and PM_1 were measured over two seasons in classrooms representing different school year groups. Particle deposition fractions in the respiratory tract, as well as the deposited doses, were calculated using the Multiple-Path Particle Dosimetry (MPPD) and the Exposure Dose Model (ExDoM2). Both models were implemented assuming an 8-hour exposure scenario to represent the school day. In general, differences in PM concentrations were observed depending on room occupancy periods and season. The highest mean $PM_{2.5}$ concentration was recorded in winter when the classroom was vacant (23.7 ± 20.5 μg m^{-3}), while the highest mean PM_{10} level was observed in spring during school hours (61.7 ± 24.2 μg m^{-3}). Regardless of the dosimetry model, the highest deposition of PM_{10} and $PM_{2.5}$ was in the upper region, while the lowest was in the tracheobronchial (TB) region. The results indicate that deposited dose and deposition fraction in spring may be more harmful to pupils' health than in winter. PM_{10} presented

the highest doses, ranging from 54.2 to 128 μg and from 83.9 to 185 μg, according to MPPD and ExDoM2 estimates, respectively.

Keywords

Schoolchildren; Particulate matter; Dose; PM deposition; Dosimetry models.

1. Introduction

According to a recent report on air pollution and child health, nearly 600,000 children aged 5–15 years died from exposure to unhealthy levels of ambient and household air pollution in 2016 (WHO, 2018). Only in Europe, air pollution causes more than 1,200 deaths in people under the age of 18 every year (EEA, 2023). PM is the principal component of indoor and outdoor air pollution and includes a range of particle sizes (Lee et al., 2021). Several studies have suggested that the primary exposure mechanism of PM is inhalation, which exacerbates respiratory symptoms in patients with chronic airway diseases (Leikauf et al., 2020). PM is mostly absorbed through the respiratory tract, where it can infiltrate the lung alveoli and reach the bloodstream. In the respiratory system, PM induces the activation of alveolar macrophages and neutrophils that release reactive oxygen or nitrogen species. Oxidative stress stimulates the production of mediators of pulmonary inflammation and begin or foster numerous illnesses (Thangavel et al., 2022). Short-term exposure to particulate matter with aerodynamic diameter lower than 2.5 μm ($PM_{2.5}$) and its respiratory tract depositions are dose-responsive and related to higher blood pressure, prevalence of prehypertension and hypertension among children (Liu et al., 2021). There is also evidence that prenatal exposure to $PM_{2.5}$ and its components increases the risk of preterm birth (Shi et al., 2024). In addition, poor air quality in school buildings also contributes to health problems and can affect children's concentration and cognitive development (Sunyer et al., 2015). According to the study by Martins et al. (2020), concentrations of PM were often higher inside than outside the microenvironments evaluated in Lisbon (Portugal), with children being exposed to much higher concentrations of PM at school than at home. Faria et al. (2020) showed that although children spend more time at home than at school during weekdays, the classroom was the microenvironment that most contributed to the daily inhaled dose of $PM_{2.5}$ and PM_{10} in Lisbon. Madureira et al. (2015) found that indoor air pollutants in primary schools located in Porto (Portugal) were related to greater odds of wheezing in children. Branco et al. (2020) also reported that high exposure to $PM_{2.5}$ and O_3 in nurseries and primary schools in urban and rural areas in northern Portugal was associated with a reduction in lung function among children.

In order to evaluate pupils' exposure to air pollutants in the school environment, many studies have been carried out on the assessment of indoor and outdoor air in primary schools or nurseries in both urban and rural areas, focusing mainly on investigating the

effects related to ventilation in classrooms, evaluating comfort parameters, and carrying out the chemical characterisation of indoor and outdoor atmospheric pollutants (e.g., Abhijith et al., 2022; Almeida Sousa et al., 2021; Mainka et al., 2015; Mumovic et al., 2009). Especially in Portugal in the last four years, some studies have investigated potential sources of particulate matter in classrooms (Madureira et al., 2016), the relationship between allergy symptoms and indoor air quality in schools (Branco et al., 2020; Szabados et al., 2022), and inhaled doses of particulate matter (Faria et al., 2020), but only a few aimed to calculate PM deposition among children (Chalvatzaki et al., 2020a; Madureira et al., 2020). Although the regional deposition and dose of particles deposited in the respiratory tract are an important factor in understanding the health effects of aerosol particles (Goel et al., 2018; Linell et al., 2023), it is still unknown how size segregated PM is deposited in regions of the respiratory system and the dose deposited by children while attending classes, even when previous studies reported adverse effects related to particle deposition in the airways. For example, it was documented that the deposition of $PM_{2.5}$ increases the risk of severity of pulmonary tuberculosis in the upper and middle lobes (Makrufardi et al., 2023). In the study carried out by Kesavachandran et al. (2015), the deposition of fine particles in the airways resulted in a decline in forced expiratory volume and peak expiratory flow among outdoor exercisers. Therefore, the development of dosimetry models is an important step in understanding exposure-dose-response relationships for PM and can help in evaluating the human health effects of inhaling toxic substances in different environments (Chalvatzaki and Lazaridis, 2015). Different dosimetry modelling approaches have been broadly used to predict particle deposition and dose in human airways, such as the MPPD and the ExDoM2, for which estimates can be made for monodisperse and polydisperse aerosols, in a user-interactive environment. For example, Chalvatzaki et al. (2021) carried out simulations with ExDoM2 considering three study cases with seasonal and diurnal variations in Greek cities. Overall, a higher daily deposited dose was obtained in the cold period compared to the warm periods for all sites. This finding was associated with increased deposition rate in the cold period during the afternoon/evening, because of significant heating emissions. Recently, Khan et al. (2022)carried out MPPD simulations for a city in India and found that the mass deposited in winter was significantly greater than in monsoons for PM_1, $PM_{2.5}$ and PM_{10}, mainly due to the higher PM levels in winter.

As deposition fractions and doses may vary from season to season and there are very few studies on the deposited dose of PM while children attend classes, the current work aimed to assess winter and spring indoor levels of PM_1, $PM_{2.5}$ and PM_{10} during school hours to investigate: i) temporal variability of mass concentrations and, ii) hourly and seasonal variations in the deposition of total and regional fractions and doses of PM in the children's respiratory system using two dosimetry models.

2. Material and methods

2.1. Study area

Estarreja is a small town of about 7,000 inhabitants located in northern Portugal. The town has an important chemical complex, comprising 30 companies in an area of 290 ha, which is home to various economic sectors, such as heavy industry, retail, warehousing, and services (Alves et al., 2023). This study was carried out at a school in the north side of the town, close to the industrial complex. In addition to kindergarten, this school integrates the first two cycles of basic education. In Portugal, basic education comprises 3 stages: 1st cycle (1st to 4th grades, ages 6-9 years), 2nd cycle (5th and 6th grades, 10-11 years) and 3rd cycle (7th to 9th grades, 12-14 years).

The school of this study is surrounded by low-rise buildings, a road with little traffic, and a railway line to the west. It consists of 3 main buildings, each one dedicated to a different level of education: 1) preschool, 3 – 5 years, 2) 1st cycle, 6 – 10 years, and 3) 2nd cycle, 10 – 12 years. Buildings 1, 2 and 3 are composed of 6, 12 and 7 classrooms, respectively. To cover the different age groups and the various types of school activities, a classroom was selected in each of the buildings. By imposition of the school principal, classrooms with children with special educational needs or disabilities were considered ineligible. The general characteristics of the classrooms were: concrete walls, wooden windows, and floor, white painted and whiteboard with markers. All of them depend only on natural ventilation with windows and exterior doors.

The school is open from 7:30 to 18.30. However, the school day starts at 8:30 and finishes at 15:30. Every child is entitled to a 60-minute school lunch. In general, cleaning takes place between 16:00 and 18:00. In this study, class time corresponds to the school day considering the lunch break.

2.2. Experimental set-up and instrumentation

Measurements took place over two seasons. The winter campaign was performed between November and December 2022, and the spring campaign between April and May 2023. However, for this study, fifteen days of monitoring during each season were considered after checking the amount of complete data for each working day and in every classroom. The monitoring equipment was installed at a height of around 1 m above the floor, and at least 1 m away from any doors, windows, and walls. The indoor instruments were removed from the room and transferred to another in the next building at the end of every Friday afternoon (**Table 1**). PM_{10} simultaneous concentrations were rectified against in-situ gravimetric PM_{10} measurements.

Table 1

Sampling campaign characteristics.

Location	Description	Measurement periods
Indoor, ground floor	Kindergarten; room attended by the same class (20 pupils); age group between 3 and 5 years.	Nov. 14 – 18, 2022 April 13 – 21, 2023
Indoor, ground floor	1st cycle, 1st grade; room attended by the same class (17 kids); age group between 6 and 7 years.	Nov. 18 – 25, 2022 April 21 – 28, 2023
Indoor, 1st floor	2nd cycle, 5th and 6th grades; room attended by different classes (on average 22 children per class); age group between 10 and 11 years.	Nov. 25 – Dec. 02, 2022 April 28 – May 05, 2023

Simultaneous measurements of PM_{10}, $PM_{2.5}$, and PM_1 were obtained using an aerosol spectrometer (Grimm Model EDM 164) operated at a 1-minute time resolution. In this spectrometer, each particle is detected in the optical measuring cell and based on the intensity of the scattered light signal it is assigned a size. This model measures particle size distributions within the range from 0.25 to 32.0 µm. In addition, gravimetric PM_{10} samples were collected on 15 cm quartz microfibre filters using a high-volume sampler at an airflow rate of 500 l/min (HVS, Model CAV-A/MSb, MCV S.A).

The high-volume sampler was intercompared with real-time measurements. The regression slopes for the results obtained from parallel measurements during the two monitoring campaigns were 0.95 and 0.75, with correlation coefficients (R^2) of 0.91 and 0.95 for winter and spring, respectively. However, as there was no gravimetric equipment for fine particles, PM_1 and $PM_{2.5}$ data were corrected from the ratios obtained between the initial concentrations of PM_1/PM_{10} and $PM_{2.5}/PM_{10}$ and multiplied by the concentrations of corrected PM_{10}, in accordance with the method applied by Cipoli et al. (2022).

2.3. Estimation of particle deposition and deposition dose in the respiratory system of pupils using two models

- The MPPD model (V3.04, ARA Inc.)

The MPPD model calculates breathing from transport, deposition, and clearance in the respiratory tract of rats and humans based upon a multiple-path method (Asgharian and Anjilvel, 1998; Asgharian et al., 2001). In general, this model can predict both deposition in a typical path per airway generation (single-path) and particle deposition in all ways of the lung (multiple-path). The model provides specific human lung geometry for 10 different ages. It has three major applications: risk assessment, drug delivery and threat

assessment. In this study, MPPD was used for risk assessment. Lung geometries for ages 3, 8 and 9 were selected because of the age of children attending the school. The model input parameters are presented in four categories: inhalant properties (aerosol), airway morphometry, exposure condition and deposition/clearance settings. For aerosol properties, the density and distribution were assumed to be 1 g cm^{-3} and single, respectively, while equations 1 and 2 (Hinds and Zhu, 2022) were employed to calculate the Mass Median Aerodynamic Diameter (MMAD) and the Geometric Standard Deviation (GSD) using the mass size distribution of PM_1, $PM_{2.5}$ and PM_{10} obtained in both seasons to derive the hourly values for all classrooms (Table S1, Supplementary Material):

$$MMAD = e^{\frac{\sum c_i(\ln(d_i))}{\sum c_i}} \quad (1)$$

$$GSD = e^{\sqrt{\frac{\sum c_i(\ln(d_i)-\ln(MMAD))^2}{\sum c_i}}} \quad (2)$$

where c_i is the mass fraction in GRIMM channel i and d_i is the cut-off diameter of GRIMM channel i.

For airway morphometry, the age-specific 5-lobe was chosen and the default values for Upper Respiratory Tract (URT) and Functional Residual Capacity (FRC) were obtained from the model. Exposure was considered constant and the parameters for this category included the inspiratory fraction (value of 0.5), the Breathing Frequency (BF) and Tidal Volume (TV) that were also provided by the model, while concentrations were calculated for each of the three selected classrooms and each season considering weekdays only. In addition, since the aim of the study was to evaluate particle deposition while children were in their classrooms, only the sitting activity pattern was contemplated, and the associated breathing pattern was nasal (Patterson et al., 2014). The selection of the nasal route assumed that the study population (pupils) was sitting most of the time (low-intensity activity) and breathing spontaneously through the nose. The input parameters for each age are shown in **Table 2**, and seasonal averages of PM concentration, MMADs and GSDs are presented in Table S1, Supplementary Material.

MPPD calculates the deposition fraction based on mathematical equations described in detail by Asgharian et al. (2001). Based on the estimated concentration of DF and PM, the dose rate is calculated for each region of the respiratory tract and a report with the results is provided to the user. In this study, the period between 8 and 16 h represents the school day, therefore, dose rates were calculated for 1-hour exposure intervals and the sum of hourly doses is equivalent to the school day.

- The ExDoM2 model

ExDoM2 was also used for the calculation of deposition fraction and dose profile for the school day. The model calculates the deposition dose, clearance, and retention of aerosol particles in the human respiratory tract based on the International Commission on Radiological Protection (ICRP) human respiratory tract model. ExDoM2 allows the user to set variable or static exposure conditions, such as exposure concentration, physical exertion levels, and different environments (Chalvatzaki and Lazaridis, 2015). Furthermore, the model works with monodisperse or polydisperse aerosol size distributions where the user has the flexibility to introduce the aerosol size parameters as median aerodynamic diameter and geometric standard deviation or to quantify these values directly from the model using as input the measurement data. For a detailed description of the model see Chalvatzaki and Lazaridis (2015) and Lazaridis (2023). **Table 2** displays the values of the physiological variables used in the deposition calculations in the models.

Table 2

Input parameters according to the study group and model, applicable at normal conditions of sitting breathing.

Age	URT (ml)		FRC (ml)		BF (min^{-1})		TV (ml)	
(years)	MPPD	ExDoM2	MPPD	ExDoM2	MPPD	ExDoM2	MPPD	ExDoM2
3	9.47	nd	48.2	nd	24	nd	121.3	nd
5	nd	13.3	nd	767	nd	25	nd	213
8	21.0	nd	501.3	nd	17	nd	278.2	nd
9	22.4	nd	683.0	nd	17	nd	295.8	nd
10	nd	25	nd	1484	nd	19	nd	333

[nd] indicates missing values when that age is not considered in the model.

In general, the input parameters required in each model are similar. However, while ExDoM2 considers wind speed and automatically selects physiological parameters based on the reference values provided in the ICRP66 model, MPPD offers the user the option of directly insert these values or select the model's default values that change according to the morphology of the lung and the person's age (**Table 3**). Both models consider age as an input parameter, but the selection options differ from one model to another. In ExDoM2 the user can choose between 5 options that consider gender (1 year, 5 years, 10 years, 15 years, or adults), while with MPPD, the user has the option to choose one of the following ages: 3 months, 21 months, 23 months, 28 months, 3 years, 8 years, 9 years, 14 years, 18 years, or 21 years. Additionally, different from MPPD, in ExDoM2 the user must specify the gender of the individual. The respective ages used in this study are presented according to the model in Table S2, Supplementary material.

Table 3

Model specifications according to input options.

Parameter	Entered by user	Select from a list of options	Automatically set by the model

PM concentration	Both models		
Density	Both models		
MMAD	Both models		
GSD	Both models		
Wind speed	ExDoM2 only		
Exposure scenario		Both models	
Activity level		Both models	
URT	MPPD only		ExDoM2 only
FRC	MPPD only		ExDoM2 only
BF	MPPD only		ExDoM2 only
TV	MPPD only		ExDoM2 only
Total lung capacity			Both models
Age		Both models	
Gender		ExDoM2 only	

The same input data for the implementation of MPPD for each group was used as input in the ExDoM2: (1) mean hourly PM concentration, (2) breathing pattern, (3) particle density, (4) hourly MMADs and GSDs, and (5) shape factor. The hourly wind speed was only considered in ExDoM2, and it was calculated for each classroom from data obtained during the winter monitoring campaign (Table S3, Supplementary material). In addition, in ExDoM2 model, the simulations were also implemented for each gender, female and male.

In addition to using a very different approach, another difference between the models is related to the presentation of the results. While MPPD provides an output report, the ExDoM2 model estimates the dose by formula (3), and generates an output file that includes hourly doses, making it necessary to isolate the DF in equation 3:

$$Dose\ (\mu g\ h^{-1}) = PM_i * DF_{i,j} * VT \quad (3)$$

where PM_i is the mean exposure concentration of PM in the size fraction i (μg m^{-3}), $DF_{i,j}$ is the deposition fraction in the region j of the respiratory tract for PM in the size fraction i, and VT is the ventilation per hour ($m^3\ h^{-1}$) of the exposed pupil, depending on age. To represent the school day, dose rates were calculated for a total of 8 h exposure duration in 1 h exposure time intervals.

2.4. Data analysis

For the treatment and analysis of the PM concentrations, a minimum data availability of 75% per school day was considered. After checking the normality of the data, PM concentrations were examined with typical descriptive statistics including measures of central tendency and dispersion, diurnal cycles, highlighting the school period and significant differences between seasons and between the time of occupancy versus non-

occupancy with the non-parametric Wilcoxon test, where a p-value <0.05 was considered statistically significant.

Subsequently, the data from the dosimetry models were analysed separately and then the results of the two models were combined, considering the size of the PM and the groups evaluated to extract the general behaviour of the deposited fractions and doses. Association, agreement, and comparison analyses were performed using linear regression, Bland-Altman method, and t-test for paired samples.

3. Results and discussion

3.1. General overview of PM concentrations

Median concentrations of PM_{10} varied from 6.7 to 24.4 μg m^{-3} in winter, and between 13 and 18 μg m^{-3} in spring. As shown in **Table 4**, the median concentrations of PM_{10}, $PM_{2.5}$ and PM_1 in the room attended by 2nd cycle students were 1.3, 1.2 and 1.4 times higher in winter. PM levels were higher in winter in the 2nd cycle room, while PM concentrations were higher in spring in kindergarten and 1st cycle room. In general, PM concentrations were statistically different between the two seasons in all classrooms.

Table 4
Median of PM concentrations (μg m^{-3}) for weekdays in each classroom in winter and spring.

	Winter			Spring		
Classroom	PM_{10}	$PM_{2.5}$	PM_1	PM_{10}	$PM_{2.5}$	PM_1
Kindergarten						
Median	6.67	6.05	4.42	14.0	12.5	10.0
IQR_a	15.6	3.07	1.10	15.8	1.93	5.15
1st cycle						
Median	18.1	9.96	6.31	18.1	15.0	11.4
IQR	21.6	5.76	3.06	39.6	3.99	2.62
2nd cycle						
Median	24.5	15.7	13.8	18.7	13.0	9.21
IQR	24.9	14.8	16.1	8.79	4.17	5.82

[a]Interquartil range.

To compare PM concentrations in the school environment, the hourly average concentration for PM is shown in **Fig.1**. The highest and lowest PM_{10} hourly concentration was recorded in two different seasons. While the maximum value was observed in the 1st cycle room (128 μg m^{-3}; 16:00) in spring, the lowest concentration was recorded in the kindergarten (4.9 μg m^{-3}; 7:00) in winter. PM_{10} concentrations in both seasons showed the main peaks during class time and periodic cleaning hour, which can be explained because the rooms are normally swept, in addition to the resuspension of soil material brought in on the soles of shoes, emissions associated with student

activities (e.g., paper and clothing fibres, skin peeling) and infiltration from outside to the classroom environment, as reported in other studies (Alves et al., 2013; Madureira et al., 2016). $PM_{2.5}$ represented, on average, 35% and 31% of the PM_{10} concentrations during class time compared to 91% and 90% during unoccupied periods in winter and spring, respectively.

The **Fig. 1** also revealed that $PM_{2.5}$ and PM_1 concentrations in the 1st and 2nd cycle rooms in winter began to increase almost at the end of the school day and, depending on the classroom, reached their peak between 18:00 and 22:00, which may suggest the penetration of particles from residential biomass combustion. A different pattern was observed in the kindergarten room, where the concentration of fine particles did not increase at night. It is believed that this behaviour is because the door always remains closed after cleaning hours, making it difficult for particles to penetrate the environment, as reported by other authors (Long et al., 2001). In a sampling campaign carried out in a nearby school between September and November, it was concluded, based on the chemical speciation of $PM_{2.5}$, that biomass combustion represented 9% of the mass concentrations (Alves et al., 2023). In the present study, it is expected that the contribution from this source will be greater, since it was carried out in winter, with lower temperatures. In spring, concentrations for both particle sizes remained almost constant throughout the day, with mean values below 15 and 11 μg m^{-3} for $PM_{2.5}$ and PM_1, respectively.

Although the daily mean concentrations were not higher than the values recommended by the World Health Organisation (PM_{10}: 45 and $PM_{2.5}$:15 μgm^{-3}), in winter, hourly PM_{10} concentrations above 45 μg m^{-3} were observed in the kindergarten and the 1st cycle room, with a maximum of 62.7 μg m^{-3} during the school day. In spring, the peaks were registered in the kindergarten and the 1st cycle room between 11:00 and 15:00, while the 2nd cycle room did not record concentrations above 45 μg m^{-3} at any time of the day. Regarding $PM_{2.5}$, hourly concentrations above 15 μg m^{-3} were recorded in both the 1st and 2nd cycle rooms, with levels in the 1st cycle room varying from 15.5 to 23.5 μg m^{-3} between 6:00 and 16:00 in spring.

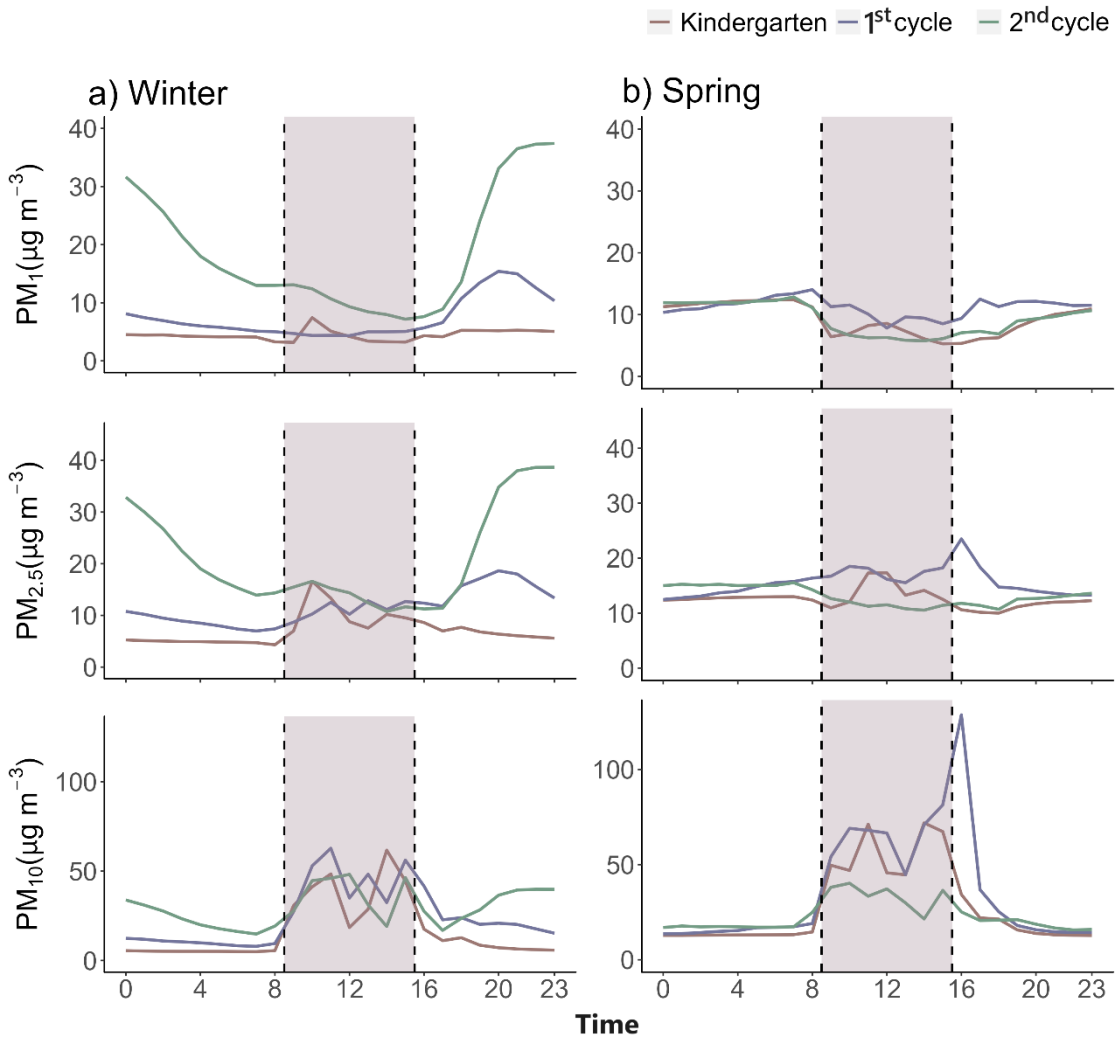

Figure 1. Variation in hourly average PM concentrations during weekdays in a) winter and b) spring. The highlighted band represents the class time.

According to the difference between the 5th and 95th percentiles (**Fig. 2**), there was greater variability in $PM_{2.5}$ and PM_1 concentrations in winter than in spring, mainly when the classrooms were not occupied. On the other hand, PM_{10} concentrations varied more in class time than unoccupancy periods in the two seasons. In general, much higher PM_{10} concentrations were observed during the school day compared to concentrations measured during the period when classrooms were vacant. The maximum difference was recorded in spring when the average concentration in the kindergarten classroom was 17.2 µg m^{-3} during school hours and rose up to 51.7 µg m^{-3} when the classroom was vacant. Unlike PM_{10}, PM_1 concentrations were higher during free periods than class hours in both winter and spring, except in the 1st cycle room. $PM_{2.5}$ concentrations between class time and unoccupancy periods in the kindergarten were similar in winter and spring, while in the 1st cycle room, class time levels were higher in spring.

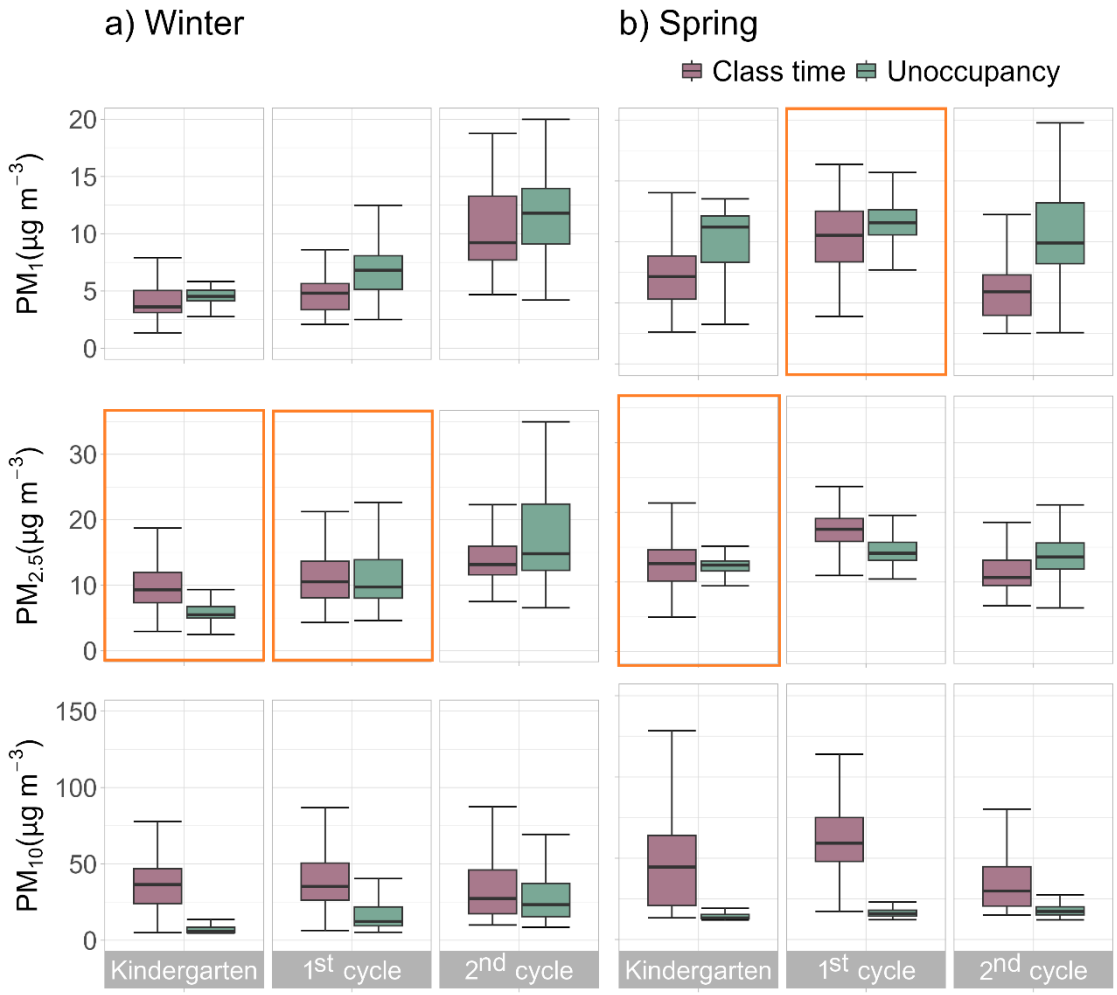

Figure 2. Box plots showing the concentrations of particulate matter in class time and rest of the day in each room for a) winter and b) spring. Lower and upper boundaries of box plots represent the 25th and 75th percentiles, respectively; the line represents median values. The highlighted orange frames indicate when concentrations were not statistically different between school day and unoccupancy periods.

In this study, the average concentrations of PM_{10} and $PM_{2.5}$ considering the two seasons and all classrooms were 3.82 and 3.16 times lower than those reported by Branco et al. (2019) in nurseries and primary schools in urban and rural locations in the north of Portugal. Some studies have shown that student activities increase PM generation indoors. Martins et al. (2020) reported that children in Lisbon were exposed to significantly higher concentrations of PM at school than at home, and that indoor concentrations of PM_{10} and $PM_{2.5}$ were often higher than outdoors. According to researchers, human activity and external infiltration are the main sources associated with internal PM. However, the results of the Lazović et al. (2022) study indicate that the average concentrations of PM_{10} and $PM_{2.5}$ in the outdoor environment in primary schools in Serbia were 20% and 32% higher than the concentrations observed in classrooms. Therefore, PM concentrations can be affected by several factors, such as classroom

activities, ventilation, occupancy rate and external sources (Alameddine et al., 2022; Tippayawong et al., 2009).

3.2. Deposition fraction of PM in two seasons and using two deposition models

Deposition fractions were obtained for the school day using two models (**Table 5**). In general, for all groups and in both seasons, the deposition fractions of $PM_{2.5}$ and PM_{10} in the various regions of the respiratory tract showed the following trend: tracheobronchial < pulmonary < head airway. This is in line with the trends reported in previous studies (Jia et al., 2021; Khan et al., 2022).

Overall, there were small differences between spring and winter DFs, as DFs do not depend on PM concentrations (Sánchez-Soberón et al., 2015), as previously reported in studies using MPPD (Li et al., 2015). In this study, the total DF of PM_{10} calculated with MPPD and ExDoM2 was up to 4% and 7% higher in spring than in winter, respectively. This behaviour was slightly different for the finer particles (PM_1 and $PM_{2.5}$), being mainly larger in winter, except for children from the 2nd cycle, for whom DF were 4% and 10% higher in spring according to MPPD and ExDoM2, respectively (**Table 5**). The seasonal DF of PM_{10} and $PM_{2.5}$ was identified to be associated with the mass mean aerodynamic diameter, as reported by Manojkumar and Srimuruganandam (2022) in the city of Vellore, India. Based on the data from this study and using both models, it was possible to observe that larger MMADs led to greater DF, regardless of the children's age. This indicates that the DF varies with the particle properties and, therefore, is normally not directly proportional to the mass concentration, as reported in the results of the study by Kumar et al. (2017).

Table 5. Average deposition fractions for the different PM sizes during a school day.

	MPPD				**ExDoM2**			
Winter	**Head**	**TB**	**P**	**Total**	**Head**	**TB**	**P**	**Total**
PM_1								
Kindergarten	0.22	0.03	0.13	0.39	0.12	0.02	0.09	0.23
1st cycle	0.23	0.04	0.17	0.44	0.07	0.02	0.08	0.17
2nd cycle	0.21	0.04	0.18	0.43	0.04	0.03	0.08	0.15
$PM_{2.5}$								
Kindergarten	0.26	0.03	0.16	0.45	0.37	0.02	0.13	0.52
1st cycle	0.26	0.04	0.23	0.52	0.25	0.02	0.14	0.41
2nd cycle	0.24	0.04	0.17	0.44	0.09	0.02	0.09	0.21
PM_{10}								
Kindergarten	0.33	0.09	0.24	0.66	0.73	0.03	0.08	0.84

1st cycle	0.32	0.12	0.30	0.74	0.63	0.04	0.11	0.78
2nd cycle	0.34	0.16	0.18	0.68	0.56	0.03	0.10	0.69
Spring								
PM_1								
Kindergarten	0.21	0.04	0.14	0.39	0.07	0.03	0.09	0.18
1st cycle	0.21	0.04	0.19	0.43	0.04	0.03	0.08	0.15
2nd cycle	0.21	0.04	0.17	0.43	0.05	0.03	0.08	0.15
$PM_{2.5}$								
Kindergarten	0.25	0.03	0.15	0.43	0.30	0.02	0.12	0.44
1st cycle	0.25	0.03	0.19	0.47	0.15	0.02	0.11	0.28
2nd cycle	0.25	0.04	0.19	0.48	0.17	0.02	0.12	0.31
PM_{10}								
Kindergarten	0.35	0.10	0.24	0.69	0.79	0.03	0.07	0.89
1st cycle	0.35	0.14	0.26	0.75	0.69	0.04	0.10	0.82
2nd cycle	0.34	0.14	0.24	0.72	0.63	0.03	0.10	0.77

TB: tracheobronchial; P: Pulmonary.

Still according to **Table 5**, the fraction in the head was the highest of the total airway deposition, representing up to 35% with MPPD and 79% with ExDoM2. However, this pattern was not observed for PM_1, when using the ExDoM2 model, especially in spring, since in all ages the highest value was observed in the lung region and not in the head. This can be because particles with a larger mass median aerodynamic diameter deposit more in the head region, while smaller aerodynamic diameters deposit preferably in the alveolar region, considering that deposition by Brownian diffusion occurs mainly in the acinar region of the lung (Darquenne, 2020), Although with MPPD the greatest contribution was not from the head, the fraction of PM_1 deposition in the alveolar region was higher when compared to the fractions of PM_{10} and $PM_{2.5}$.

In general, the main difference between the models occurs for smaller particles. ExDoM2 calculates higher total DF of PM_{10} but lower values for $PM_{2.5}$ and PM_1. MPPD calculates higher DF in TB and pulmonary regions, while ExDoM2 estimates higher values for the head airway region. This is mainly due to discrepancies in the morphometry data such as airway lengths, diameters, and branching angles, which in turn depend on the choice of the lung model and the input values of the respiratory variables, such as URT and FRC. For example, ExDoM2 uses average values from different models (Weibel, 1963; Yeh and Schum, 1980; Phalen et al., 1985; Hansen and Ampaya, 1975) that vary depending on the respiratory region (Aleksandropoulou and Lazaridis, 2013), but MPPD considers 8 geometries of the human lung, with the user being responsible for choosing one of the options. In addition, the models use different approaches for deposition calculations. While ExDoM2 is mainly based on the empirical equations proposed in ICRP, MPPD is

based on that proposed by Asgharian and Anjilvel. (1998), also using a Monte Carlo approach.

The smallest variation between the total deposition results of the models was observed for the 2nd cycle, whereas the largest difference between the models was identified in kindergarten. The total DF of PM_{10} estimated with the ExDoM2 was up to 22% higher than the results from MPPD. However, the total DF of $PM_{2.5}$ and PM_1 derived from MPPD was higher (up to 66% for PM_1) than the value estimated with ExDoM2 in both seasons (Table S4, Supplementary material). By way of example, **Fig. 3** displays the diurnal cycles of deposition fraction of particulate matter in the group of 9- and 10-year-old children, split into sizes and model. It is possible to observe little difference from one model to another in the total DF of PM_{10}, although there are large differences in the DF by regions.

It is noticeable in **Fig. 3** that a larger fraction of PM_1 and $PM_{2.5}$ is deposited in the lung region, while PM_{10} is deposited in the head region. ExDoM2 predictions show DFs of $PM_{2.5}$ of 0.09 in the head and lung, while the fraction of PM_{10} deposited in the upper airway and pulmonary region averaged 0.56 and 0.10, respectively. MPPD follows the same trend but with different values. While the fraction of $PM_{2.5}$ deposited in the head and P was, on average, 0.24 and 0.17, respectively, the fraction of PM_{10} deposited in head and P was, on average, 0.34 and 0.19, respectively. This trend was also observed by Gao et al. (2022) in a study carried out in China with 10-year-old children during commuting trips to school, which showed that for the three transport modes evaluated and the three particle sizes, the proportion of DFs in the head was the highest, especially for PM_{10}, representing up to more than 85% of the total fraction deposited. For PM_1 and $PM_{2.5}$, the DFs of the P significantly exceeded those of the TB part. This is especially important since children with asthma are more sensitive to air pollution because they breathe at higher tidal volumes, which can increase the efficiency of $PM_{2.5}$ deposition in the lung (Afshar-Mohajer et al., 2022).

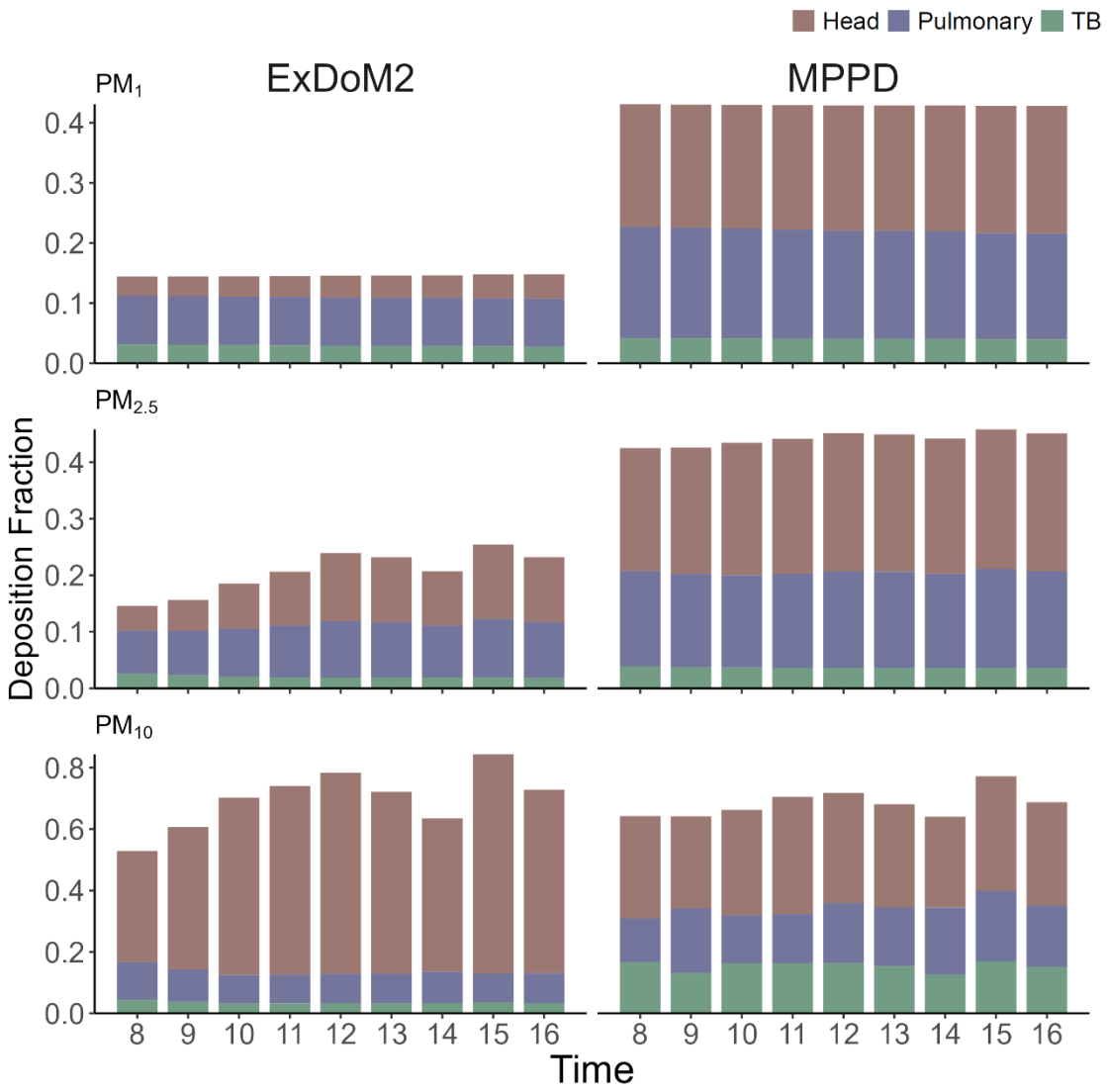

Figure 3. Hourly deposition fraction for different particle sizes in children aged 10 years (ExDoM2) and 9 years (MPPD) during the school day in winter. DFs were calculated from average values during a week of measurements in December.

After the comparison of both models, it was observed that the deposition of particles larger than 1.17 μm was greater than that of smaller particles. Location wise, it was greater in the head region due to their higher sedimentation and impaction rates, while the deposition of particles with smaller sizes was greater in the P region due to the diffusion effect (Guo et al., 2019). Overall, this trend was most noticeable with the ExDoM2 results, which can be explained because the respiratory tract model (RTM) used in ExDoM2 is an updated version of the RTM (ICRP, 2012), in which particles deposited in the extrathoracic region (ET) are partitioned 65% to ET1 and 35% to ET2 (Chalvatzaki and Lazaridis, 2015).

3.3. Deposition dose during the school day

Fig. 4 shows the deposited dose during the school day of the three sizes of PM in different parts of the respiratory system for all children in the two periods evaluated. Important differences can be observed between the two seasons and the two models, with values being higher in spring. While seasonal variations showed only a slight influence on the total deposition fraction, they had a large effect on the school day deposited dose, particularly during spring as a direct consequence of higher PM concentrations (Table S5, Supplementary material). On the other hand, after calculating the deposited dose and the deposition fraction considering the gender of the children, it was observed that regardless of their age, the results were the same for both girls and 5-year-old boys, and likewise for girls and boys aged 10 years. This may be because ExDoM2 uses as input the same values for physiological parameters without differentiating by gender. For this reason, the results in this study were always reported and discussed for children according to age, and not by gender.

The highest accumulated dose of $PM_{2.5}$ and PM_{10} in the two seasons occurred for children attending the 1st cycle and coincides with the highest environmental concentration of PM_1 and $PM_{2.5}$ observed in this room. The overall results show that while the total PM_{10} deposition dose estimated with ExDoM2 was up to 58% higher than the values derived from the MPPD model, the dose for PM_1 obtained with the MPPD was between 15% and 69% higher than the value calculated with ExDoM2. The differences can be attributed to the specific values used in the two models for the tidal volume and respiratory frequency parameters and, consequently, the value of the ventilation rate. Furthermore, the increase and decrease in dose estimated in any of the models coincides with the observed pattern in the deposition fraction (**Fig. 4**).

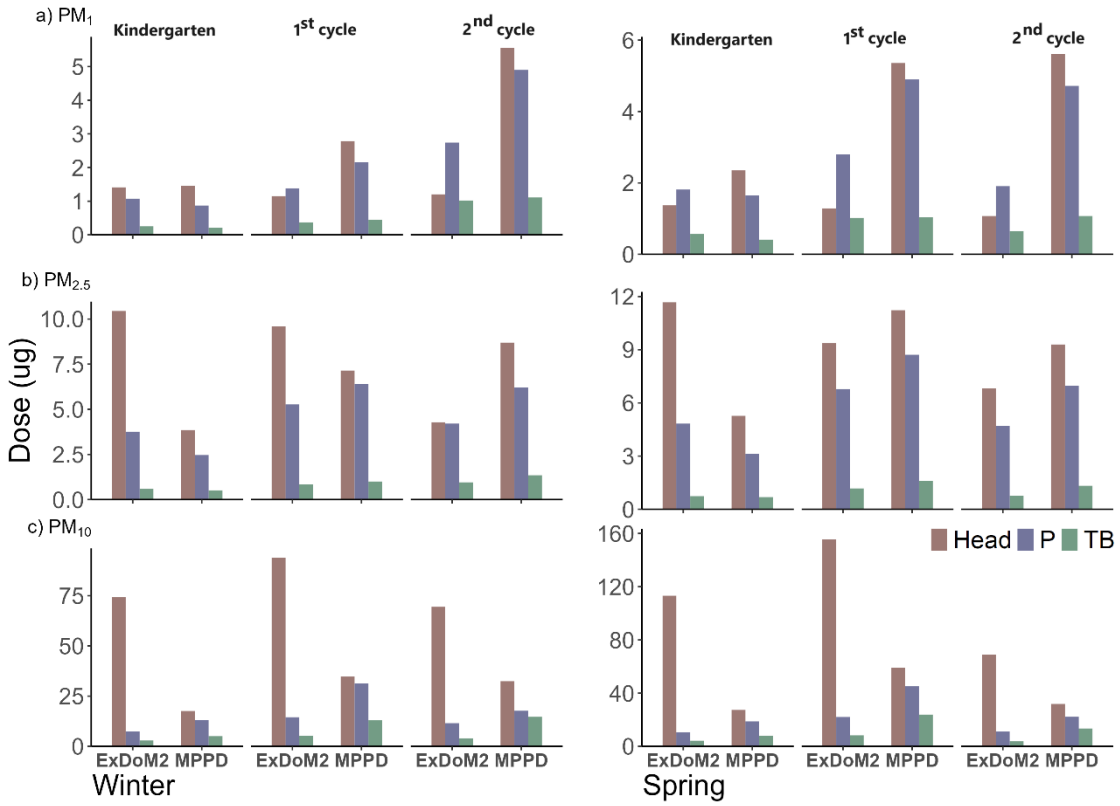

Figure 4. Regional deposited dose of a) PM_1, b) $PM_{2.5}$ e c) PM_{10} for each group during the school day in winter and spring. Comparison between the two models. Head: upper airway; P: pulmonary; TB: tracheobronchial. Different scales on the y-axis were purposely chosen to highlight the values and aid visualisation.

The PM_{10} doses for the school day calculated in the present study were lower than the results reported in previous studies. Chalvatzaki et al. (2020) applied ExDoM2 to predict the PM_{10} dose received by students at five primary schools in Lisbon, Portugal, assuming that the exposed children were 10-year-old nasal breathers. The researchers found that the total deposited dose ranged from 72 to 239 μg in indoor school environments, while in the current study it was, on average, 84.4 μg with the same model (10 years old) and 66 μg with MPPD (9 years old). Faria et al. (2020) quantified the exposure of children between 5 and 10 years old to PM and the respective daily inhaled dose considering various microenvironments in Lisbon. The researchers observed that during the week children inhale, on average, 96 and 177 μg of $PM_{2.5}$ and PM_{10}, respectively, with the classroom contributing more than the residential environment. In their study, the inhaled doses were higher than the doses calculated with both models in this study, as the inhaled dose does not consider the deposition fraction and, therefore, the estimated value will always be higher. In any case, these results showed that children inhale more PM in classrooms than in residential environments, despite spending more time at home.

Regarding the amount of PM deposited per region, higher cumulative doses occurred mainly in the head region and lower ones in the TB region, except for PM_1 calculated with ExDoM2 (**Fig. 4**), coinciding with the pattern of deposition fractions. However, unlike the DFs of PM_1 (ExDoM2) from kindergarten in winter, the DFs of PM_1 with ExDoM2 were always greater in the lung region than in the upper airways. This can be associated with the aerodynamic diameter of the particles, since when compared by classrooms and seasons, the largest MMADs of PM_1 obtained was in kindergarten in winter (Table S1, Supplementary Material). However, even though the DFs of PM_1 (ExDoM2) were higher in the lung region, they were lower than the values estimated with the MPPD.

In general, a comparison between the two models revealed that higher deposition doses in the lung and TB region were always estimated with MPPD for 8- and 9-year-old children in both seasons. Nevertheless, the same did not happen in kindergarten due to the ventilation rate in ExDoM2 being 0.095 $m^3 h^{-1}$ higher than the value used by MPPD, despite the DFs calculated with MMPD for these two regions being always higher than those estimated with ExDoM2. In both seasons, the majority of the PM_{10} dose was deposited in the head region, while PM_1 and $PM_{2.5}$ were predominantly deposited in the lung region. It is noteworthy that different mechanisms govern PM deposition in the TB and lung regions, such as diffusion, impaction, and sedimentation (Deng et al., 2018). Regardless of the model, special attention should be paid to these results, particularly those related to finer particles, since $PM_{2.5}$ depositions in the respiratory tract, including P and TB regions, are associated with elevated blood pressure and greater risk of prehypertension and hypertension in children aged 4 to 12 years (Liu et al., 2021).

Fig. 5 shows a statistical summary of the hourly deposited doses of PM_1, $PM_{2.5}$ and PM_{10} for all groups between 8 h and 16 h. With MPPD, a 3-year-old child has a lower mean dose deposited per hour compared to children aged 8 and 9 years for the three PM sizes evaluated in both seasons, while with ExDoM2, the lowest values were observed in children aged 10 years of the 2nd cycle. The differences observed in deposited doses can be explained by the DFs predicted by the two models. In the case of MPPD, deposition efficiency is lower in the respiratory tract of 3-year-old children compared to 8- and 9-year-old children, whatever the particle size and season, while ExDoM2 predictions showed the highest DF values for 5-year-old children. As shown by Poorbahrami et al. (2021), the differences in total and regional deposition calculations are probably due to the use of different lung models, which in turn suggest volumetric and structural differences in lung morphologies according to the ages of the individuals.

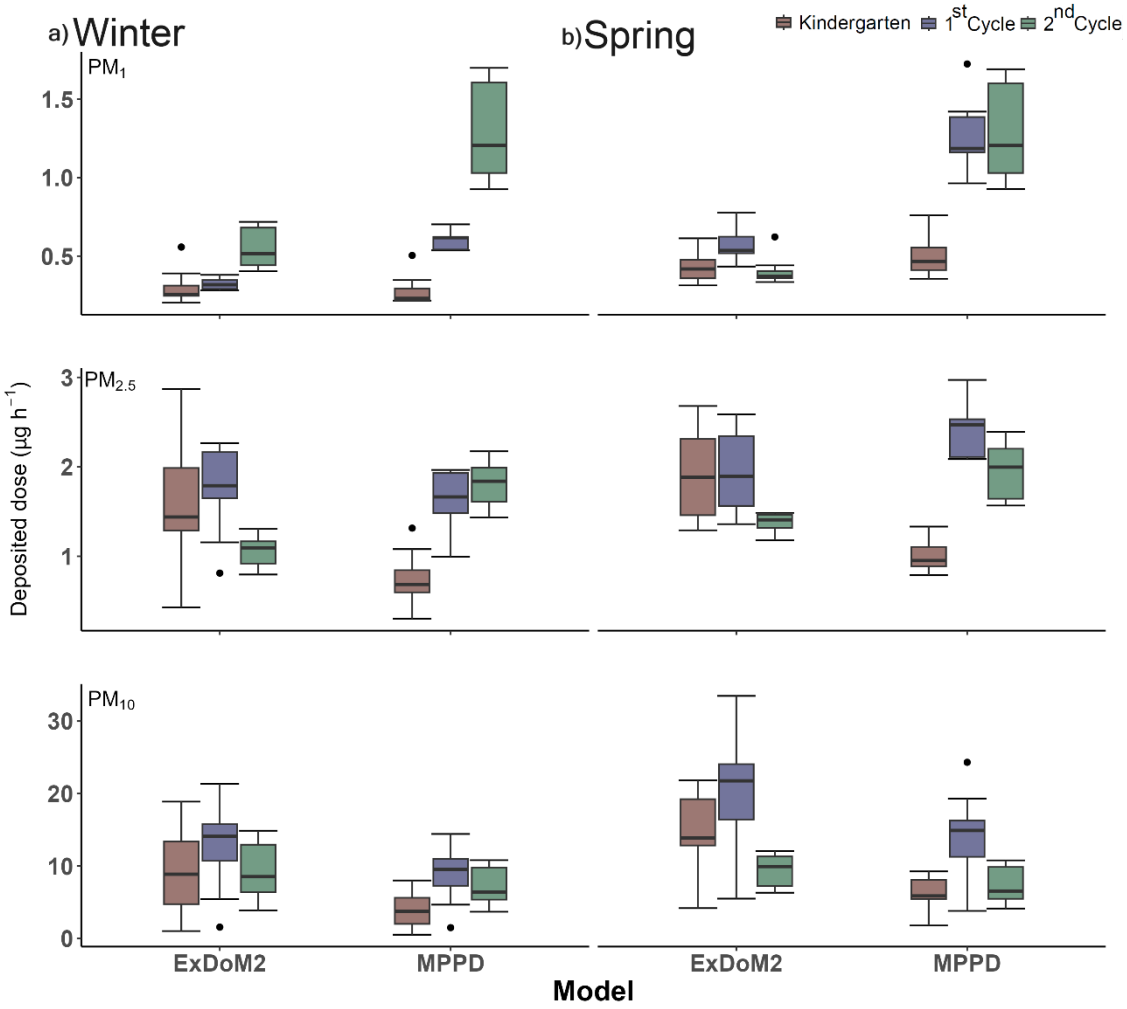

Figure 5. Boxplots with hourly doses of different sizes of PM for the three groups evaluated, split into model and a) winter and b) spring.

Although both models describe the same hourly profile pattern, with peaks at different times depending on classroom activities and particle size, the deposited dose values show clear differences from model to model. In the 1st cycle and 2nd cycle classrooms, the $PM_{2.5}$ and PM_{10} peaks coincided at the same time, different from the PM_1 pattern, with more stable values being observed throughout the day. The hourly profile for winter reveals that both particle doses calculated with ExDoM2 and those estimated from MPPD showed variations linked to PM sources (**Fig. 6)**. Normally, the deposited dose increased between 8 h and 10 h (which is related to the start of the school day) and decreased during rest and lunch times. On the other hand, high doses, generally from 14 h onwards, are associated with students leaving, as well as emissions from cleaning classrooms.

The difference between the PM_{10} doses predicted by ExDoM2 were 58%, 31% and 24% higher than those calculated with the MPPD for kindergarten, 1st cycle and 2nd cycle, respectively, while for PM_1 the MPPD calculated doses 46% and 57% higher for children

in the 1st cycle and 2nd cycle, respectively. This is in accordance with the pattern of the total deposition fraction of these PM sizes and their respective concentrations. However, despite the MPPD calculating higher DFs for PM_1 and $PM_{2.5}$ in kindergarten and 1st cycle compared to ExDoM2, the doses did not follow this behaviour. This is due to the ventilation rate used by ExDoM2 being higher, compared to the values used by MPPD for children aged 3 and 8 years. Similar relationships were also observed in spring.

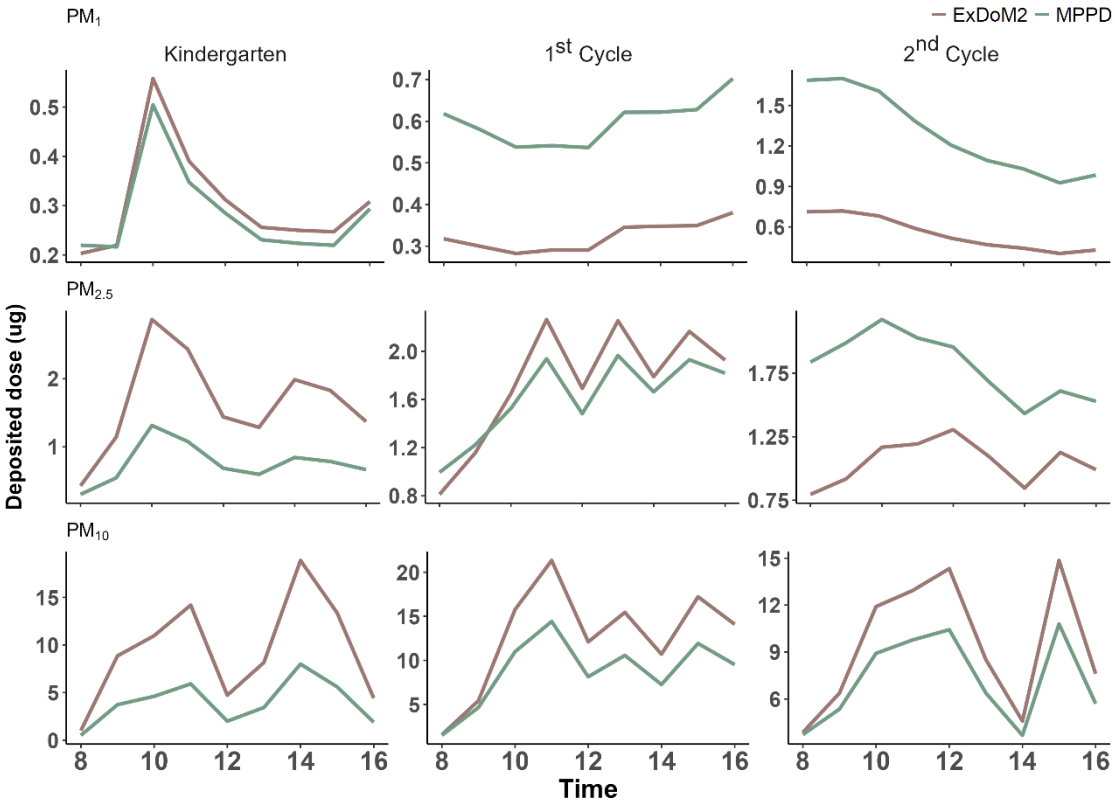

Figure 6. Hourly cycle of PM deposition doses during school hours in winter according to group and the dosimetry model.

Furthermore, high R values (R> 0.89) were observed between the MPPD and ExDoM2 hourly doses in both seasons (Table S6, Supplementary Material). However, there were some exceptions, as in the case of the 2nd cycle classroom. The low correlations occur because some dose peaks calculated with MPPD were not present in the ExDoM2 dataset or because one of the models showed lower doses compared to the other. Coincidentally, weak correlations between the hourly doses of the two models were observed only for R values below 0.63 between hourly deposited dose and hourly exposure (Table S5, Supplementary Material).

In addition to linear regression, the difference and agreement between the hourly doses of the two models were also evaluated. While the paired t-test applied at a significance level of 5% revealed that there are statistically significant differences in the hourly

deposited dose of all PM sizes in the two seasons, the Bland-Altman test confirmed that even though there were differences in the hourly values, good agreement was found between the predictions of the two models for deposited particle doses (Table S7 and Figure S1, Supplementary Material.

Overall, this study highlights the importance of evaluating the personal exposure to PM of children of different ages who attend a large school that integrates several levels of education (~700 students), and which is located less than 1 km away from the largest industrial complex in the country. In Portugal, schools offering pre-school, 1st cycle and 2nd cycle education are abundant (10,991 establishments) and represent 71% of the population of children attending these levels of education (~1,189,353 students from pre-school up to the 3rd cycle of basic education). Thus, the results of this study may be valid in other establishments with these levels of education, and serve to encourage measurements in school environments considering a larger group of classes to calculate in more detail the exposure of schoolchildren to PM. However, the results should be interpreted with caution because they are based on a short data set that may have been affected by specific conditions of the sampling period or by sporadic events. The impossibility of monitoring and collecting samples simultaneously in different classrooms and other school environments constitutes another limitation of the study. In addition, variability in the activities carried out in the classrooms was not considered. Therefore, the children's respiratory patterns were constant, and the same exposure scenario was evaluated (nasal breathing under sitting activity level). Finally, whenever possible, monitoring in classrooms for longer periods (more than 1 week) should be taken into account, as well as carrying out at least one sampling campaign in each season with the aim of improving the representation of variations in weather conditions and school activities throughout the academic year.

4. Conclusions

This study suggests that PM concentrations are statistically different from one season to another, and that the variability of concentrations is also influenced by room occupancy periods, with higher levels of PM_{10} during the school day compared to periods when the classrooms are empty. Although PM levels were low compared to other studies, dosimetry models indicate that a significant amount of PM was deposited in pupils' respiratory tracts during school hours. The patterns indicate larger deposited doses in spring compared to winter, with children aged 9 and 10 attending the 1st cycle being the most affected. Furthermore, the variations observed in the deposition fractions and deposited doses for the models are the result of differences in the physiological parameters of the respiratory system (e.g., URT, FRC, BF and TV) used as input, which are age dependent. None of the models covers all ages of the children targeted in the

present study. In general, a good agreement was obtained between both models, although some differences, especially for regional deposition, could be observed. The dosimetry models applied in this research may be useful in other educational settings to identify and mitigate the impact of local and regional sources of air pollution in the school environment.

Declaration of Competing Interest

The authors declare that they have no known competing financial interests or personal relationships that could have influenced the work documented in this manuscript.

Acknowledgements

The authors would especially like to thank the school principal, teachers, parents, and children who have willingly participated in this study. The help of Prof. Teresa Nunes, from the Department of Environment at the University of Aveiro, in interpreting the data is also appreciated. Special thanks to Owen Price from Applied Research Associates, Inc. for his support and expertise in answering questions related to MPPD. The authors acknowledge the financial support of the Portuguese Foundation for Science and Technology (FCT) to CESAM (UIDP/50017/2020+UIDB/50017/2020+ LA/P/0094/2020), through national funds, and to the PhD fellows I. Charres (SFRH/BD/2022.12142), Y. Cipoli (SFRH/BD/04992/2021), L. Furst (SRFH/BD/08461/2020) and I. Rienda (SFRH/BD/144550/2019). FCT is also acknowledged for the research contract under Scientific Employment Stimulus to Estela D. Vicente (DOI:10.54499/2022.00399.CEECIND/CP1720/CT0012). This work was performed within the STEP project - Schools Tackling Estarreja's Air Pollution – funded by the LabEx-DRIIHM-OHM programme (CNRS – INEE, France).

Appendix A. Supplementary material. Additional material related to this paper is available online at:

References

Abhijith, K.V., Kukadia, V., Kumar, P., 2022. Investigation of air pollution mitigation measures, ventilation, and indoor air quality at three schools in London. Atmos Environ 289, 119303. https://doi.org/10.1016/j.atmosenv.2022.119303

Afshar-Mohajer, N., Wu, T.D., Shade, R., Brigham, E., Woo, H., Wood, M., Koehl, R., Koehler, K., Kirkness, J., Hansel, N.N., Ramchandran, G., McCormack, M.C., 2022. Obesity, tidal volume, and pulmonary deposition of fine particulate matter in children with asthma. European Respiratory Journal 59. https://doi.org/10.1183/13993003.00209-2021

Aleksandropoulou, V., Lazaridis, M., 2013. Development and application of a model (ExDoM) for calculating the respiratory tract dose and retention of particles under variable exposure conditions. Air Qual Atmos Health 6. https://doi.org/10.1007/s11869-010-0126-z

Almeida Sousa, N., Segalin, B., Buse, A., Filho, W., Fornaro, A., Gonçalves, F., 2021. Indoor/outdoor particulate matter and health risk in a nursing community home in São Paulo, Brazil. Atmos Pollut Res 12.

Alves, C., Evtyugina, M., Vicente, E., Vicente, A., Rienda, I.C., de la Campa, A.S., Tomé, M., Duarte, I., 2023a. PM2.5 chemical composition and health risks by inhalation near a chemical complex. Journal of Environmental Sciences 124, 860–874. https://doi.org/10.1016/j.jes.2022.02.013

Alves, C., Evtyugina, M., Vicente, E., Vicente, A., Rienda, I.C., Sánchez De La Campa, A., Tomé, M., Duarte, I., 2023b. PM 2.5 chemical composition and health risks by inhalation near a chemical complex. journal of environmental sciences 124, 860–874. https://doi.org/10.1016/j.jes.2022.02.013

Alves, C., Nunes, T., Silva, J., Duarte, M., 2013. Comfort Parameters and Particulate Matter (PM10 and PM2.5) in School Classrooms and Outdoor Air. Aerosol Air Qual Res 13, 1521–1535. https://doi.org/10.4209/aaqr.2012.11.0321

Asgharian, B., Anjilvel, S., 1998. A multiple-path model of fiber deposition in the rat lung. Toxicological Sciences 44. https://doi.org/10.1006/toxs.1998.2476

Asgharian, B., Hofmann, W., Bergmann, R., 2001. Particle deposition in a multiple-path model of the human lung. Aerosol Science and Technology 34. https://doi.org/10.1080/02786820119122

Branco, P.T.B.S., Alvim-Ferraz, M.C.M., Martins, F.G., Ferraz, C., Vaz, L.G., Sousa, S.I.V., 2020a. Impact of indoor air pollution in nursery and primary schools on childhood asthma. Science of The Total Environment 745, 140982. https://doi.org/10.1016/j.scitotenv.2020.140982

691 Branco, P.T.B.S., Alvim-Ferraz, M.C.M., Martins, F.G., Ferraz, C., Vaz, L.G., Sousa,
692 S.I.V., 2020b. Impact of indoor air pollution in nursery and primary schools on
693 childhood asthma. Science of The Total Environment 745, 140982.
694 https://doi.org/10.1016/j.scitotenv.2020.140982

695 Chalvatzaki, E., Chatoutsidou, S.E., Kopanakis, I., Melas, D., Parliari, D.,
696 Mihalopoulos, N., Lazaridis, M., 2021. Personal deposited dose and its influencing
697 factors at several Greek sites: an analysis in respect to seasonal and diurnal
698 variations. Environmental Science and Pollution Research 28, 29276–29286.

699 Chalvatzaki, E., Chatoutsidou, S.E., Martins, V., Faria, T., Diapouli, E., Manousakas,
700 M., Almeida, S.M., Eleftheriadis, K., Lazaridis, M., 2020a. Assessment of the
701 Personal Dose Received by School Children due to PM10 Air Pollution in Lisbon.
702 Aerosol Air Qual Res 20, 1384–1397. https://doi.org/10.4209/aaqr.2020.01.0022

703 Chalvatzaki, E., Chatoutsidou, S.E., Martins, V., Faria, T., Diapouli, E., Manousakas,
704 M., Almeida, S.M., Eleftheriadis, K., Lazaridis, M., 2020b. Assessment of the
705 Personal Dose Received by School Children due to PM10 Air Pollution in Lisbon.
706 Aerosol Air Qual Res 20, 1384–1397. https://doi.org/10.4209/aaqr.2020.01.0022

707 Chalvatzaki, E., Lazaridis, M., 2015. Development and application of a dosimetry
708 model (ExDoM2) for calculating internal dose of specific particle-bound metals in
709 the human body. Inhal Toxicol 27, 308–320.
710 https://doi.org/10.3109/08958378.2015.1046201

711 Cipoli, Y.A., Targino, A.C., Krecl, P., Furst, L.C., Alves, C. dos A., Feliciano, M.,
712 2022. Ambient concentrations and dosimetry of inhaled size-segregated particulate
713 matter during periods of low urban mobility in Bragança, Portugal. Atmos Pollut
714 Res 13, 101512. https://doi.org/10.1016/j.apr.2022.101512

715 Darquenne, C., 2020. Deposition mechanisms. J Aerosol Med Pulm Drug Deliv 33,
716 181–185.

717 Deng, Q., Ou, C., Chen, J., Xiang, Y., 2018. Particle deposition in tracheobronchial
718 airways of an infant, child and adult. Science of the Total Environment 612.
719 https://doi.org/10.1016/j.scitotenv.2017.08.240

720 European Environment Agency, 2023. Harm to human health from air pollution in
721 Europe: burden of disease 2023.

722 Faria, T., Martins, V., Correia, C., Canha, N., Diapouli, E., Manousakas, M.,
723 Eleftheriadis, K., Almeida, S.M., 2020a. Children's exposure and dose assessment
724 to particulate matter in Lisbon. Build Environ 171, 106666.
725 https://doi.org/10.1016/j.buildenv.2020.106666

726 Faria, T., Martins, V., Correia, C., Canha, N., Diapouli, E., Manousakas, M.,
727 Eleftheriadis, K., Almeida, S.M., 2020b. Children's exposure and dose assessment

to particulate matter in Lisbon. Build Environ 171, 106666. https://doi.org/10.1016/j.buildenv.2020.106666

Gao, J., Qiu, Z., Cheng, W., Gao, H.O., 2022. Children's exposure to BC and PM pollution, and respiratory tract deposits during commuting trips to school. Ecotoxicol Environ Saf 232. https://doi.org/10.1016/j.ecoenv.2022.113253

Goel, A., Izhar, S., Gupta, T., 2018. Study of environmental particle levels, its effects on lung deposition and relationship with human behaviour. Environmental Contaminants: Measurement, Modelling and Control 77–91.

Guo, J., Ji, A., Wang, J., Ogunseitan, O.A., Xu, Z., 2019. Emission characteristics and exposure assessment of particulate matter and polybrominated diphenyl ethers (PBDEs) from waste printed circuit boards de-soldering. Science of the Total Environment 662. https://doi.org/10.1016/j.scitotenv.2019.01.176

Hinds, W.C., Zhu, Y., 2022. Aerosol technology: properties, behavior, and measurement of airborne particles. John Wiley & Sons.

Jia, S., Zhang, Q., Yang, L., Sarkar, S., Krishnan, P., Mao, J., Hang, J., Chang, M., Zhang, Y., Wang, X., Chen, W., 2021. Deposition of ambient particles in the human respiratory system based on single particle analysis: A case study in the Pearl River Delta, China. Environmental Pollution 283. https://doi.org/10.1016/j.envpol.2021.117056

Kesavachandran, C.N., Kamal, R., Bihari, V., Pathak, M.K., Singh, A., 2015. Particulate matter in ambient air and its association with alterations in lung functions and respiratory health problems among outdoor exercisers in National Capital Region, India. Atmos Pollut Res 6, 618–625.

Khan, S., Gurjar, B.R., Sahu, V., 2022. Deposition modeling of ambient particulate matter in the human respiratory tract. Atmos Pollut Res 13, 101565.

Kumar, P., Rivas, I., Sachdeva, L., 2017. Exposure of in-pram babies to airborne particles during morning drop-in and afternoon pick-up of school children. Environmental Pollution 224. https://doi.org/10.1016/j.envpol.2017.02.021

Lazaridis, M., 2023. Modelling approaches to particle deposition and clearance in the human respiratory tract. Air Qual Atmos Health 16, 1989–2002. https://doi.org/10.1007/s11869-023-01386-1

Lee, Y.G., Lee, P.H., Choi, S.M., An, M.H., Jang, A.S., 2021. Effects of air pollutants on airway diseases. Int J Environ Res Public Health. https://doi.org/10.3390/ijerph18189905

Leikauf, G.D., Kim, S.H., Jang, A.S., 2020. Mechanisms of ultrafine particle-induced respiratory health effects. Exp Mol Med. https://doi.org/10.1038/s12276-020-0394-0

765 Li, X., Yan, C., Patterson, R.F., Zhu, Yujiao, Yao, X., Zhu, Yifang, Ma, S., Qiu, X.,
766 Zhu, T., Zheng, M., 2015. Modeled deposition of fine particles in human airway in
767 Beijing, China. https://doi.org/10.1016/j.atmosenv.2015.06.045

768 Linell, J., Isaxon, C., Olsson, B., Stroh, E., Wollmer, P., Löndahl, J., Rissler, J., 2023.
769 Effects of breathing variables on modelled particle lung deposition at physical
770 activity for children and adults. Air Qual Atmos Health 1–14.

771 Liu, M., Guo, W., Zhao, L., Yang, H., Fang, Q., Li, M., Shu, J., Chen, S., Lai, X., Yang,
772 L., Zhang, X., 2021. Association of personal fine particulate matter and its
773 respiratory tract depositions with blood pressure in children: From two panel
774 studies. J Hazard Mater 416. https://doi.org/10.1016/j.jhazmat.2021.126120

775 Long, C.M., Suh, H.H., tros Kout, P.J.C. and P., 2001. Using Time- and Size-Resolved
776 Particulate Data To Quantify Indoor Penetration and Deposition Behavior. Environ
777 Sci Technol 35. https://doi.org/10.1021/es011283d

778 Madureira, J., Paciência, I., Rufo, J., Ramos, E., Barros, H., Teixeira, J.P., de Oliveira
779 Fernandes, E., 2015. Indoor air quality in schools and its relationship with
780 children's respiratory symptoms. Atmos Environ 118.
781 https://doi.org/10.1016/j.atmosenv.2015.07.028

782 Madureira, J., Paciência, I., Rufo, J., Severo, M., Ramos, E., Barros, H., de Oliveira
783 Fernandes, E., 2016. Source apportionment of CO2, PM10 and VOCs levels and
784 health risk assessment in naturally ventilated primary schools in Porto, Portugal.
785 Build Environ 96, 198–205. https://doi.org/10.1016/j.buildenv.2015.11.031

786 Madureira, J., Slezakova, K., Silva, A.I., Lage, B., Mendes, A., Aguiar, L., Pereira,
787 M.C., Teixeira, J.P., Costa, C., 2020. Assessment of indoor air exposure at
788 residential homes: Inhalation dose and lung deposition of PM10, PM2.5 and
789 ultrafine particles among newborn children and their mothers. Science of The Total
790 Environment 717, 137293. https://doi.org/10.1016/j.scitotenv.2020.137293

791 Mainka, A., Brągoszewska, E., Kozielska, B., Pastuszka, J.S., Zajusz-Zubek, E., 2015.
792 Indoor air quality in urban nursery schools in Gliwice, Poland: Analysis of the case
793 study. Atmos Pollut Res 6, 1098–1104. https://doi.org/10.1016/j.apr.2015.06.007

794 Makrufardi, F., Bai, K.-J., Suk, C.-W., Rusmawatiningtyas, D., Chung, K.F., Chuang,
795 H.-C., 2023. Alveolar deposition of inhaled fine particulate matter increased risk of
796 severity of pulmonary tuberculosis in the upper and middle lobes. ERJ Open Res 9.

797 Manojkumar, N., Srimuruganandam, B., 2022. Age-specific and seasonal deposition of
798 outdoor and indoor particulate matter in human respiratory tract. Atmos Pollut Res
799 13, 101298. https://doi.org/10.1016/j.apr.2021.101298

800 Martins, V., Faria, T., Diapouli, E., Manousakas, M.I., Eleftheriadis, K., Viana, M.,
801 Almeida, S.M., 2020. Relationship between indoor and outdoor size-fractionated

particulate matter in urban microenvironments: Levels, chemical composition and sources. Environ Res 183, 109203. https://doi.org/10.1016/j.envres.2020.109203

Mumovic, D., Palmer, J., Davies, M., Orme, M., Ridley, I., Oreszczyn, T., Judd, C., Critchlow, R., Medina, H.A., Pilmoor, G., Pearson, C., Way, P., 2009. Winter indoor air quality, thermal comfort and acoustic performance of newly built secondary schools in England. Build Environ 44, 1466–1477. https://doi.org/10.1016/j.buildenv.2008.06.014

Organization, W.H., others, 2018. Air pollution and child health: prescribing clean air: summary.

Patterson, R.F., Zhang, Q., Zheng, M., Zhu, Y., 2014. Particle Deposition in Respiratory Tracts of School-Aged Children. Aerosol Air Qual Res 14, 64–73. https://doi.org/10.4209/aaqr.2013.04.0113

Poorbahrami, K., Vignon-Clementel, I.E., Shadden, S.C., Oakes, J.M., 2021. A whole lung in silico model to estimate age dependent particle dosimetry. Sci Rep 11. https://doi.org/10.1038/s41598-021-90509-8

Sánchez-Soberón, F., Mari, M., Kumar, V., Rovira, J., Nadal, M., Schuhmacher, M., 2015. An approach to assess the Particulate Matter exposure for the population living around a cement plant: modelling indoor air and particle deposition in the respiratory tract. Environ Res 143, 10–18. https://doi.org/10.1016/j.envres.2015.09.008

Shi, T.S., Ma, H.P., Li, D.H., Pan, L., Wang, T.R., Li, R., Ren, X.W., 2024. Prenatal exposure to PM2. 5 components and the risk of different types of preterm birth and the mediating effect of pregnancy complications: a cohort study. Public Health 227, 202–209.

Sunyer, J., Esnaola, M., Alvarez-Pedrerol, M., Forns, J., Rivas, I., López-Vicente, M., Suades-González, E., Foraster, M., Garcia-Esteban, R., Basagaña, X., Viana, M., Cirach, M., Moreno, T., Alastuey, A., Sebastian-Galles, N., Nieuwenhuijsen, M., Querol, X., 2015. Association between Traffic-Related Air Pollution in Schools and Cognitive Development in Primary School Children: A Prospective Cohort Study. PLoS Med 12. https://doi.org/10.1371/journal.pmed.1001792

Szabados, M., Kakucs, R., Páldy, A., Kotlík, B., Kazmarová, H., Dongiovanni, A., Di Maggio, A., Kozajda, A., Jutraz, A., Kukec, A., Otorepec, P., Szigeti, T., 2022. Association of parent-reported health symptoms with indoor air quality in primary school buildings – The InAirQ study. Build Environ 221, 109339. https://doi.org/10.1016/j.buildenv.2022.109339

Thangavel, P., Park, D., Lee, Y.C., 2022. Recent Insights into Particulate Matter (PM2.5)-Mediated Toxicity in Humans: An Overview. Int J Environ Res Public Health. https://doi.org/10.3390/ijerph19127511

840

841
842

843

SUPPLEMENTARY MATERIAL

Table S6. Mean concentration (μg m^{-3}), MMADs (μm) and GSDs (μm) of PM_{10} used as input data in the two models.

Kindergarten		Winter			Spring	
Time	PM_{10}	MMAD	GSD	PM_{10}	MMAD	GSD
8:00	5.53	1.24	2.95	14.6	4.05	2.18
9:00	30.7	3.80	1.97	49.7	3.74	2.31
10:00	41.2	2.84	2.04	47.0	4.05	1.79
11:00	48.4	3.73	1.76	71.3	3.28	1.96
12:00	18.4	2.55	2.09	45.7	3.61	2.15
13:00	28.7	3.60	2.00	44.6	4.31	1.70
14:00	61.7	4.45	1.56	71.9	4.39	1.65
15:00	44.4	4.08	1.62	67.4	3.62	1.98
16:00	17.5	2.51	2.21	34.3	2.89	2.45
1st cycle	Winter			Spring		
Time	PM_{10}	MMAD	GSD	PM_{10}	MMAD	GSD
8:00	9.50	1.01	2.21	19.1	3.22	3.03
9:00	27.3	1.32	2.47	54.2	3.54	2.65
10:00	52.9	3.18	2.41	69.1	3.66	2.26
11:00	62.7	4.17	1.80	68.0	3.91	1.97
12:00	34.9	4.21	1.63	66.6	3.10	2.82
13:00	48.2	3.48	1.93	44.7	3.86	2.13
14:00	32.4	3.70	1.80	71.0	4.15	1.82
15:00	56.1	3.15	2.05	81.4	4.51	1.57
16:00	41.6	4.02	1.76	128.7	2.42	3.32
2nd cycle	Winter			Spring		
Time	PM_{10}	MMAD	GSD	PM_{10}	MMAD	GSD
8:00	19.2	0.98	5.41	24.9	3.19	2.81
9:00	27.7	1.70	5.82	38.1	3.49	2.37
10:00	44.6	2.78	3.86	40.2	3.28	2.47
11:00	46.0	3.08	3.25	33.4	3.53	2.34
12:00	48.2	3.40	2.73	37.3	3.29	2.32
13:00	31.1	2.81	3.20	29.9	2.53	2.45
14:00	19.1	2.00	3.99	21.5	3.64	2.13
15:00	46.4	3.90	2.25	36.5	2.64	2.89
16:00	27.5	2.85	3.06	25.1	2.17	3.22

The equations used by ExDoM2 to calculate the particle deposition for the upper respiratory tract region (DF_H), which includes the extrathoracic airways ET1 (anterior nose) and ET2 (posterior nasal passages, larynx, pharynx and mouth); the tracheobronchial region (DF_{TB}) which includes the bronchial (BB) and the bronchiolar (bb); the alveolar region (DF_{AL}) and the total deposition (DF) are those formulated by the International Commission on Radiological Protection (ICRP) and are presented below. In the equations, d_p is the particle diameter in μm, and IF is the inhalable fraction (in equations 1 and 4) and is calculated according to equation 5.

$$DF_H = IF\left[\frac{1}{1 + e^{(6.84+1.183 \ln d_p)}} + \frac{1}{1 + e^{(0.924-1.885 \ln d_p)}}\right] \quad (1)$$

$$DF_{TB} = \left(\frac{0.00352}{d_p}\right)\left[\, e^{(-0.234(\ln d_p + 3.40)^2)} + 63.9e^{(-0.819(\ln d_p - 1.61)^2)}\right] \quad (2)$$

$$DF_{AL} = \left(\frac{0.0155}{d_p}\right)\left[\, e^{(-0.416(\ln d_p + 2.84)^2)} + 19.11e^{(-0.482(\ln d_p - 1.362)^2)}\right] \quad (3)$$

$$DF = IF\left[0.0587 + \frac{0.911}{1 + e^{(4.77 + 1.485 \ln d_p)}} + \frac{0.943}{1 + e^{(0.508 - 2.58 \ln d_p)}}\right] \quad (4)$$

$$IF = 1 - 0.5\left(1 - \frac{1}{7.6x10^{-4}{d_p}^2 + 1}\right) + 10^{-5}U^{2.75}e^{(0.055 d_p)} \quad (5)$$

Table S7. Age considered according to the model.

	MPPD	ExDoM2
Kindergarten	3 years	5 years
1st cycle	8 years	10 years
2nd cycle	9 years	10 years

Thermal conditions, including wind direction, were measured with a portable monitoring equipment (Delta Ohm 32.1 and 32.3), which included the following sensors: AP3203 - Omnidirectional Hot Wire Probe, TP3275 - Globe Temperature Probe, and HP3217R - Combined Temperature and RH Probe. The equipment was installed at a height of 1 m above the floor and operated at a 1-minute time resolution. Each classroom was monitored for a week in winter 2022 (**Table S3**).

Table S8. Average wind speed (m s^{-1}).

Time	Kindergarten	1st cycle	2nd cycle
8:00 – 8:59	0.000	0.001	0.001
9:00 – 9:59	0.000	0.002	0.001
10:00 – 10:59	0.005	0.005	0.002
11:00 – 11:59	0.003	0.002	0.002
12:00 – 12:59	0.000	0.002	0.002
13:00 – 13:59	0.000	0.003	0.001
14:00 – 14:59	0.001	0.005	0.001
15:00 – 15:59	0.008	0.002	0.001
16:00 – 16:59	0.002	0.002	0.002

The discrepancies between the dosimetry models for different particle sizes in the two seasons are presented in **Table S4**. For PM_{10}, the total DF is up to 22%, showing that the MPPD

underestimates the total DF compared to the ExDoM2 counterparts. However, ExDoM2 appears to underestimate the total DF for finer particles compared to the other model.

Table S9. Discrepancy of total DFs derived from the models. Bold indicates that ExDoM2 gave values higher than MPPD.

	Winter			Spring		
	PM_{10}	$PM_{2.5}$	PM_1	PM_{10}	$PM_{2.5}$	PM_1
Kindergarten	**22%**	**13%**	41%	**22%**	**3%**	53%
1st cycle	**5%**	20%	60%	**8%**	40%	66%
2nd cycle	**2%**	53%	66%	**6%**	36%	64%

Table S10. Linear correlation coefficients between hourly exposure and hourly deposited dose according to the model (R).

	Winter						**Spring**					
	MPPD			**ExDoM2**			**MPPD**			**ExDoM2**		
	PM_{10}	$PM_{2.5}$	PM_1	PM_{10}	$PM_{2.5}$	PM_1	PM_{10}	$PM_{2.5}$	PM_1	PM_{10}	$PM_{2.5}$	PM_1
Kindergarte												
n	0.99	0.99	0.99	0.99	0.96	0.99	0.99	0.98	1	0.99	0.78	0.99
1st cycle	0.98	0.99	0.99	0.95	0.96	0.90	0.95	0.87	0.99	0.91	**0.09***	0.99
2nd cycle	0.98	0.98	1	0.97	**0.09***	0.99	**0.63***	**0.12***	**0.41***	0.92	**0.06***	0.99

*Values indicate weak correlations.

889 **Table S11**. Linear correlation coefficients between the hourly deposited doses by the two
890 models (R).

	Winter			Spring		
	PM_{10}	$PM_{2.5}$	PM_1	PM_{10}	$PM_{2.5}$	PM_1
Kindergarten	0.99	0.98	0.98	0.99	0.89	0.99
1st cycle	0.99	0.98	0.92	0.99	**0.40***	0.99
2nd cycle	0.99	**0.20***	0.99	**0.58***	**0.45***	**0.40***

891 *Values indicate weak correlation.
892
893 **Table S12**. Average hourly deposited dose of PM in each monitoring campaign and p-values
894 from the paired sample t-test. Dose values are presented in μg h^{-1} for both models.

	PM_{10}			**$PM_{2.5}$**			**PM_1**		
Campaign	**MPPD**	**ExDoM2**	**p-value**	**MPPD**	**ExDoM2**	**p-value**	**MPPD**	**ExDoM2**	**p-value**
Kindergarten -wr	3.96	9.40	1.0E-03	0.76	1.64	2.8E-04	0.28	0.31	1.11e-02
1st cycle - wr	8.77	12.6	7.2E-04	1.61	1.75	0.046	0.60	0.32	5.8E -10
2nd cycle - wr	7.20	9.44	1.2E-03	1.81	1.05	1.0E-05	1.29	0.55	2.0E-06
Kindergarten - sg	6.20	14.2	6.1E-05	1.01	1.92	1.6E-05	0.49	0.42	2.0E-04
1st cycle - sg	14.3	20.7	4.6E-05	2.40	1.93	2.8E -03	1.26	0.57	1.8E-07
2nd cycle - sg	7.49	9.32	1.3E-03	1.95	1.36	9.4E -05	1.29	0.40	7.3E-06

895 Wr: winter; sp: spring.

896 The Bland-Altman graph was generated to assess the agreement between the two models. The
897 differences between doses are displayed on the y axis; on the x-axis, dose averages are plotted.
898 This method has two limits of agreement at ±1.96 times the standard deviation. Ideally, all points
899 should fall between these two limits. After making the graphs for all rooms and the three particle
900 sizes of the two seasons, the 1st cycle room presented a point outside the limits of agreement for
901 PM_{10} and PM_1 and, the 2nd cycle room for PM_{10} in spring. The other cases were always within this
902 limit, as shown in **Figure S1**.

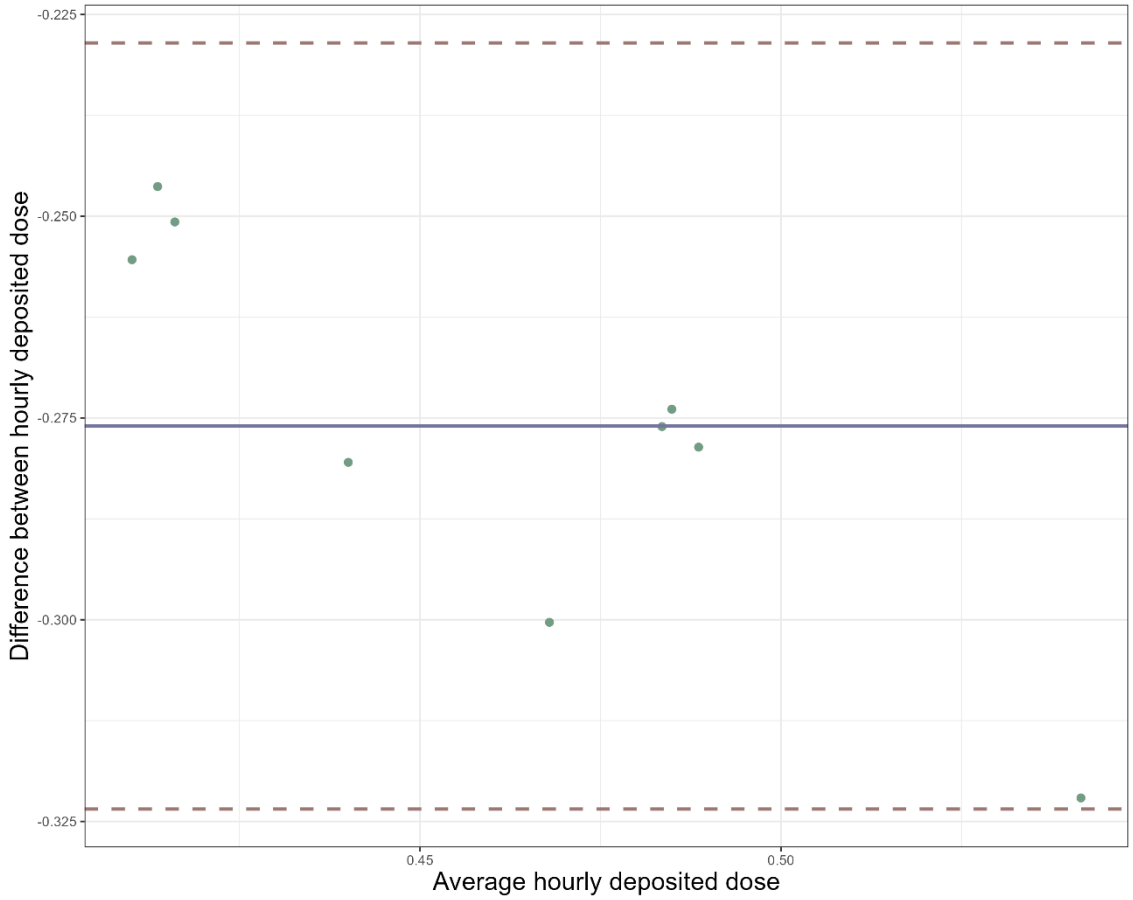

Figure S7. Bland-Altman plot generated for the hourly deposited doses of PM_1 calculated for 1st cycle in winter.

References

International Commission on Radiological Protection (ICRP) (2002). Guide for the Practical Application of the ICRP Human Respiratory Tract Model. Annals of the ICRP 32 (1-2), Pergamon, Oxford, 1 - 312